Application of a Robust Faulted Phase Selector to High-Resistance and Weak-Infeed Fault Conditions on a 1000-kV UHV Transmission Line

Renzo Fabián Espinoza, Ozenir Dias, Maria C. Tavares, and Yuri P. Molina

***Abstract*—This work proposes the use of a novel faulted phase-selection phasor-based algorithm to solve the high-resistance and weak-infeed fault condition selection problem in existent long compensated transmission lines. The algorithm was originally developed for future half-wavelength lines (3000 km for 50 Hz system or 2500 km for 60 Hz), and was slightly modified and tested in a real 645 km 1000 kV Ultra High Voltage transmission system. The algorithm was implemented in a programmable protective relay and tested using a real-time simulator. A series of tests under extreme conditions (such as high impedance fault and very week infeed system together) were conducted to evaluate the performance and robustness of the proposed algorithm.**

***Keywords*—Faulted phase selection, UHV transmission line, power system protection, weak-infeed system, high-resistance fault.**

I. Introduction

WHEN a fault occurs in the electrical power system, it should be cleared as fast as possible. For that, the protection devices need to identify the fault condition, and for proper fault loop operation, they need to identify the phases involved in the fault, specially for distance function.

High resistance (impedance) faults is a group of power system disturbances that prevent the generation of sufficient current that is required to trip the overcurrent relays, due to low fault current [1]. This kind of fault, if detected, additionally has problems to be classified. For protection functions, it is not necessary to have the fault classification, but rather the detection of the phases involved in the fault. Some research works proposed solutions for this problem [2]–[4].

Another issue is the weak-infeed. A system may be considered weak when the source impedance is high. The weak-infeed system often has relatively low values of fault current. The sequence-current-based faulted phase selectors (SCB-FPS) may have difficulties in being applied to the weak-infeed side [5].

It is possible to conclude that under extreme conditions such as high-resistance faults and weak-infeed systems, SCB-FPS algorithms have some problems, even more if both conditions appear at the same time.

A FPS algorithm for half-wavelength transmission lines (HWLs) was proposed by [6]. First studies about power transmission by means HWLs began in the USSR [7], although they should be implemented with a length that is slightly greater than half of a wavelength due to security margins for ensuring system stability [8]. These lines have yet to be constructed, however a field test was performed by transmitting 1000 VA, connecting the existing lines of the 500 kV transmission system in the USSR, and forming a transmission trunk of nearly 3000 km [9]. The test showed satisfactory results in terms of system operation.

On the other hand, the proposed HWL-FPS [6] could be applied to existing long lines, in which conventional faulted phase selector face difficulties, to correctly identify the faulted phase(s) under high-resistance and weak-infeed fault conditions. To demonstrate the applicability of this algorithm to existing real systems, a 645 km 1000-kV Ultra High Voltage (UHV) transmission system from China that was studied by [10] is used.

Parameters related to fault detection were slightly modified for the application of the proposed algorithm. In order to conduct realistic tests, the electrical system was modeled in RTDS real-time simulator and the HWL faulted phase selector was implemented in a programmable protective relay. The faults were provoked in the simulator and injected into the protective relay using an amplifier, in a hardware-in-the-loop (HIL) test system. Several tests were conducted, including weak-infeed and high-resistance fault conditions, attesting robust performance of the proposed algorithm.

The rest of this paper is structured as follows. Section 2 describes the HWL faulted phase selector algorithm proposed by [6] and the slight modification in order to be used under high-resistance and weak-infeed fault conditions. Section 3 shows the electrical system used for the tests as well as the laboratory hardware for this purpose. Section 4 shows the results of several tests conducted by means a real-time simulator and section 5 relates the mains conclusions of this work.

This study was supported by the research agencies CAPES (PNPD20130410 - 24001015062P3; code 001), CNPq and FAPESP (2017/20010-1).

R. Fabián Espinoza is with Itaipu Technological Park, PR, Brazil and with the School of Electrical Engineering, Federal University of Paraíba (UFPB), PB, Brazil; e-mail: renzo.espinoza@pti.org.br.

Yuri P. Molina are with the School of Electrical Engineering, Federal University of Paraíba (UFPB), João Pessoa, PB, Brazil; e-mail: molina.rodriguez@cear.ufpb.br.

O. Dias is with Federal University of Amazonas, Brazil; e-mail: ofdias@ufam.edu.br.

M. C. Tavares is with the School of Electrical and Computing Engineering, University of Campinas (UNICAMP), Campinas, SP, Brazil; e-mail: ctavares@unicamp.br.

Paper submitted to the International Conference on Power Systems Transients (IPST2021) in Belo Horizonte, Brazil June 17-20, 2021.

II. Faulted phase-selection algorithm

The HWL faulted phase selector (HWL-FPS) that was proposed in [6] is based on the variation of the impedances (pre-fault and in-fault) and establishes the use of three bits (`HWL_FSA`, `HWL_FSB` and `HWL_FSC`) to substitute the bits `FSA`, `FSB` and `FSC` from the sequence current based faulted phase selector (SCB-FPS) that are used by SEL protective relays. Table I shows the values that these bits must have for every shunt fault type.

TABLE I
FAULTED PHASE SELECTOR ELEMENT OUTPUTS

Bit	Fault type										
	AG	BG	CG	AB	BC	CA	ABG	BCG	CAG	ABC	ABCG
FSA	1	0	0	0	-	0	0	1	0	0	0
FSB	0	1	0	0	0	-	0	0	1	0	0
FSC	0	0	1	-	0	0	1	0	0	0	0
	Operation										
FSA	Enables AG and blocks AB and CA distance elements.										
FSB	Enables BG and blocks AB and BC distance elements.										
FSC	Enables CG and blocks BC and CA distance elements.										

A. The HWL-FPS method

The HWL-FPS studied in [6] is summarized in this subsection. The following line-to-ground and line-to-line apparent impedances are defined as:

$$Z_a = \frac{V_a}{I_a}, \quad Z_b = \frac{V_b}{I_b}, \quad Z_c = \frac{V_c}{I_c}, \\ Z_{ab} = \frac{V_{ab}}{I_{ab}}, \quad Z_{bc} = \frac{V_{bc}}{I_{bc}}, \quad Z_{ca} = \frac{V_{ca}}{I_{ca}}. \tag{1}$$

The HWL-FPS method uses the variation of these impedances considering the pre-fault and fault conditions. The Figure 1 shows the logic circuit in detail of the implemented method.

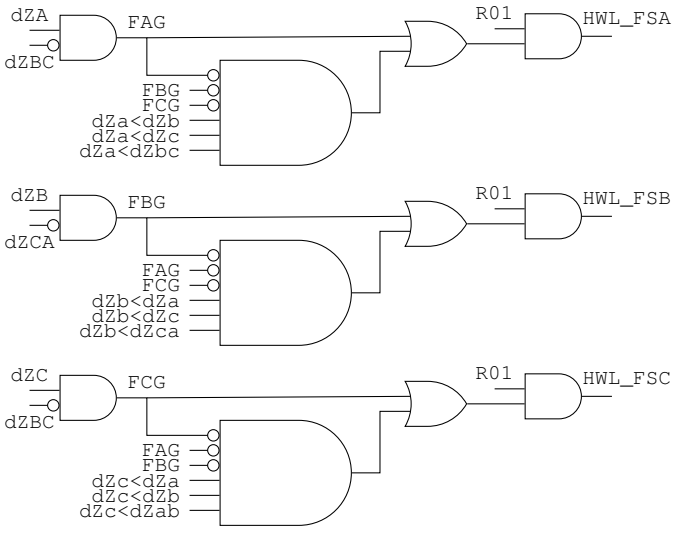

Fig. 1. The logic circuit of the HWL faulted phase selector proposed by [6], whose outputs are the bits `HWL_FSA`, `HWL_FSB` and `HWL_FSC`.

1) Line-to-ground faults: For these faults, the phase-to-phase apparent impedance corresponding to phases not involved in the fault *does not vary*. Additionally, the phase-to-ground apparent impedance corresponding to the faulted phase *varies*.

2) Line-to-Line faults: For these faults, the phase-to-ground apparent impedance corresponding to the phase not involved in the fault *does not vary*. Additionally, the phase-to-phase apparent impedance corresponding to the faulted phases *varies*.

3) Line-to-Line-to-ground faults: For these faults, the phase-to-ground apparent impedance corresponding to the phase not involved in the fault *varies less than* the other two phase-to-ground impedances. Additionally, the phase-to-phase impedance corresponding to the faulted phases *varies more than* the other two phase-to-phase impedances.

B. Proposed algorithm modification

Figure 1 shows the output bits of the HWL-FPS. This proposed algorithm can be applied to existent long compensated transmission lines connected to two strong power systems. In order to explain the operation principle described in the previous subsection, one can consider a LG (line-to-ground) fault. For this fault, there is a notorious variation in the AG impedance and the impedance BC should stay constant. Thus, the `HWL_FSA` should be activated considering this comparison. The original algorithm considers other security comparisons and it is detailed in [6]. The relation between zero sequence and positive sequence currents, and between negative sequence and positive sequence currents are used to define the fault condition. In the present study, the algorithm settings were changed slightly in order to be used under high-resistance and weak-infeed fault conditions. To increase its sensibility, the limit for detecting a fault condition was reduced from 0.15 to 0.13 according to:

$$R_{01} + R_{21} > 0.13\,; \tag{2}$$

where

$$R_{01} = \frac{|I_0|}{|I_1|}\,; \tag{3}$$

$$R_{21} = \frac{|I_2|}{|I_1|}. \tag{4}$$

Additionally, the parameter R_{01} that indicates a ground fault (bit `R01` on), was reduced from 0.1 to 0.075 according to:

$$\texttt{R01} = \begin{cases} 1, & \text{if } R_{01} > 0.075 \\ 0, & \text{otherwise} \end{cases}; \tag{5}$$

These parameters can be adjusted by the user, considering secure limits to identify a fault condition.

III. Electrical System and Laboratory Modeling for Tests

Figure 2 shows the test 1000-kV UHV transmission system used in this work. This electrical system is located in China and it was studied in [10], [11]. The electrical parameters of this 50 Hz transmission system are detailed in Tables II and III. The transmission line is 645 km in length from the Jingdongnan (JAN) to Jingmen (JEN) substations. A 1000 kV switching station (SWT) is 363 km from Jingdongnan and has shunt reactors banks.

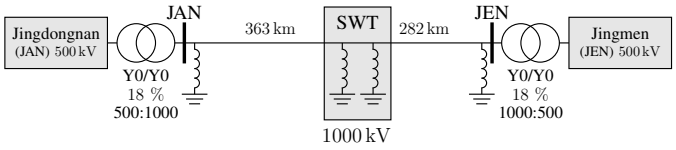

Fig. 2. Jingdongnan to Jingmen 1000-kV UHV transmission system, totalizing 645 km.

TABLE II
Substations

Substation	X_0^{min} [Ω]	X_1^{min} [Ω]	X_0^{max} [Ω]	X_1^{max} [Ω]
Jingdongnan	15.44	9.79	64.47	52.81
Jingmen	18.19	9.096	23.15	11.85

TABLE III
Transmission Line Parameters

R'_0 [Ω km^{-1}]	X'_0 [Ω km^{-1}]	B'_0 [μS km^{-1}]	R'_1 [Ω km^{-1}]	X'_1 [Ω km^{-1}]	B'_1 [μS km^{-1}]
0.20489	0.74606	2.83679	0.00805	0.25913	4.40761

The proposed algorithm was implemented on a SEL-421 programmable relay using the SELogic language [12], and tested using the RTDS real-time simulator via the hardware-in-the-loop (HIL) method, as shown in Figure 3.

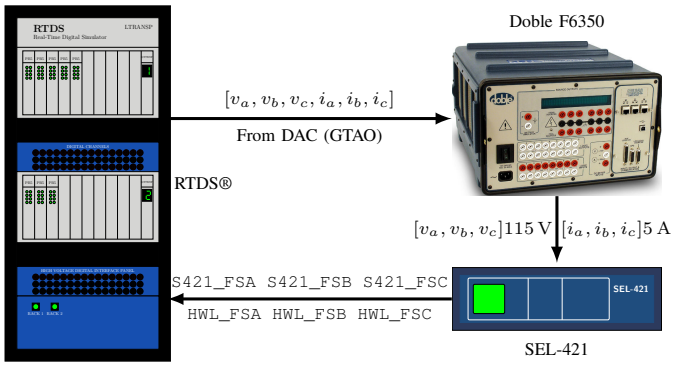

Fig. 3. Laboratory hardware-in-the-loop scheme used to test the proposed faulted phase selector algorithm. SEL-421 monitoring JAN bus.

The faulted phase selector algorithm, which was implemented on the SEL 421 programmable relay that monitors the sending terminal, was not modified, just the new limit for determining the fault condition and for activating R01 described in equations (2) and (5) was included. Additionally, the operation frequency was set to 50 Hz. All shunt fault types were applied along the transmission line considering $Rf = \{20, 60, 100, 200, 300\}$ Ω. To vary the infeed conditions, three equivalent impedances from the sending terminal were used: $Zs = \{Zs_{min}, Zs_{max}$, and $2 \times Zs_{max}\}$, for normal, weak and very weak infeed conditions, respectively. The total number of tests that were conducted was 1350, totaling over 8 hours experiment.

The laboratory hardware and its configuration were the same as those used in [6], as shown in Figure 3. So, the electrical system is modeled in the RTDS real-time simulator and the waveforms of voltage and current are injected to the protective relay by means of an amplifier, once RTDS generates low-level waveforms. At the same time, the protective relay sends the status of the all six bits to the RTDS. The three bits that correspond to the SCB-FPS native from the protective relay are named S421_FSA, S421_FSB and S421_FSC [13]. The three bits from the HWL-FPS are named HWL_FSA, HWL_FSB and HWL_FSC.

IV. Results

The Figures 4 to 7 show the oscillographies corresponding to AG fault applied in the transmission line at 272 km from JAN terminal. It is possible to see that for normal infeed condition and $R_f = 200\,\Omega$ (Figure 4) (high impedance fault), there are few variations in the voltage waveforms, and just a variation on the phase A current is observed, while the other phases currents are almost the same. For this case, the SCB-FPS and HWL-FPS operate properly. The FSA bits of both faulted phase selectors are activated and the FSB and FSC bits are in non-active status. Additionally, it is possible to see for this case that the HWL-FPS works faster than the SCB-FPS.

For the case of $R_f = 300\,\Omega$ and Normal infeed condition (Figure 5), the SCB-FPS does not work, all three bits are in non-active status. For this case, the HWL-FPS works properly activating the HWL_FSA bit and maintaining the bits HWL_FSB and HWL_FSC in non-active status. Similar behavior occurs for the case with $R_f = 200\,\Omega$ and week infeed condition (Figure 6) and for the case with $R_f = 200\,\Omega$ and very week infeed condition (Figure 7). For the last case the bit turned off for a time interval. It is possible to see that, beside the above remark, the proposed HWL-FPS works properly for all four cases, while the SCB-FPS just works properly for the first case.

The Figure 8 show a partial summary of 432 conducted tests. These figures were generated using an open-source automatic plotting tool for time-domain tests. All six bits are plotted simultaneously for every case. The bits are sorted considering time operation, from less to more. The time operation are printed in milliseconds inside the symbols. The bits are plotted taking into consideration the fault location for each case. If the bit does not operate, it will not be plotted. Line-to-line and three-line fault cases are not shown because the bits must be zero in these cases for both algorithms.

It is possible to see that under normal infeed conditions, the SCB-FPS performs properly until $Rf = 100\,\Omega$. For

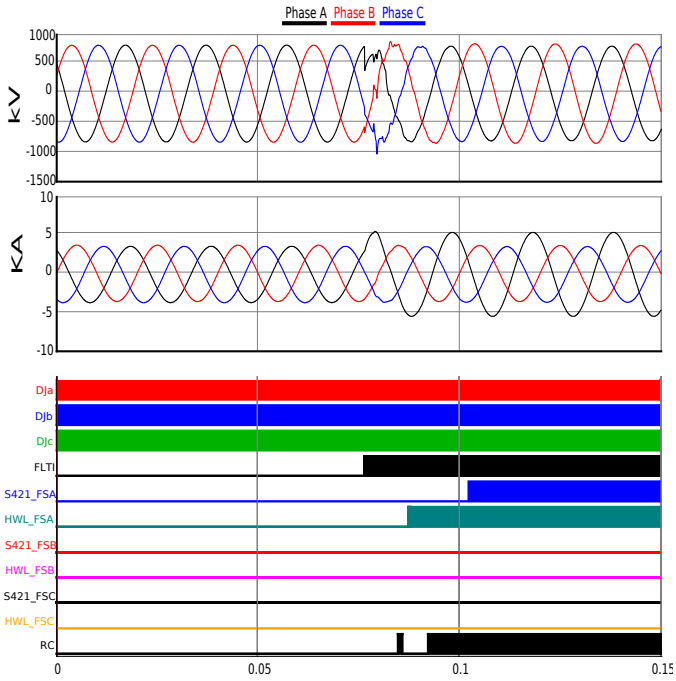

Fig. 4. Oscillography for phase A to ground fault (AG) and normal infeed condition. $Rf = 200\ \Omega$.

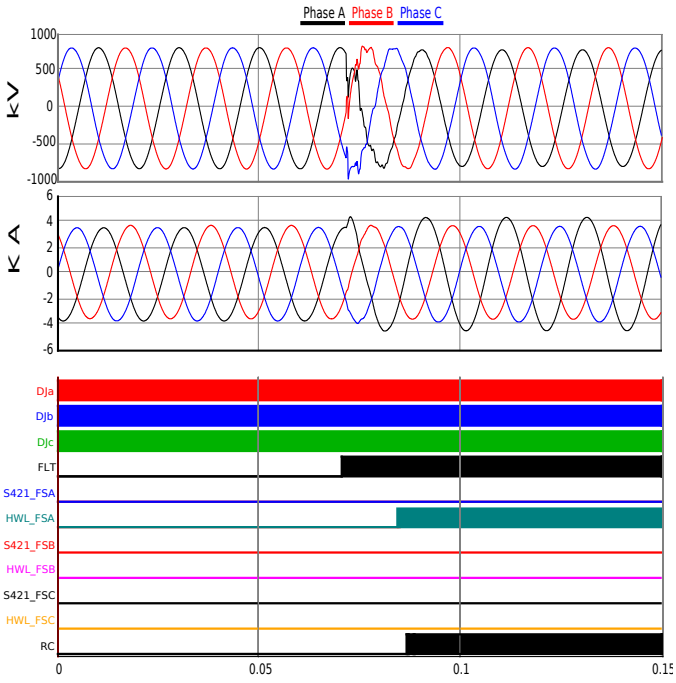

Fig. 5. Oscillography for phase A to ground fault (AG) and normal infeed condition. $Rf = 300\ \Omega$.

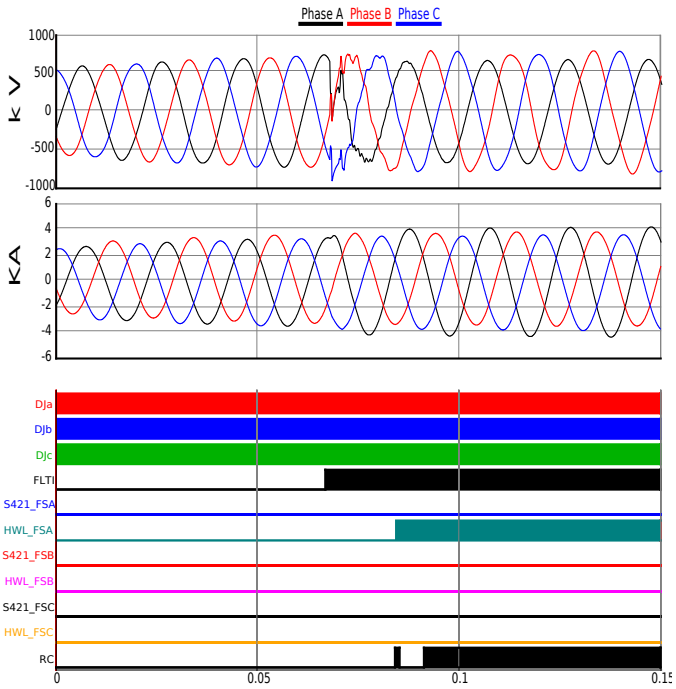

Fig. 6. Oscillography for phase A to ground fault (AG) and week infeed condition. $Rf = 200\ \Omega$.

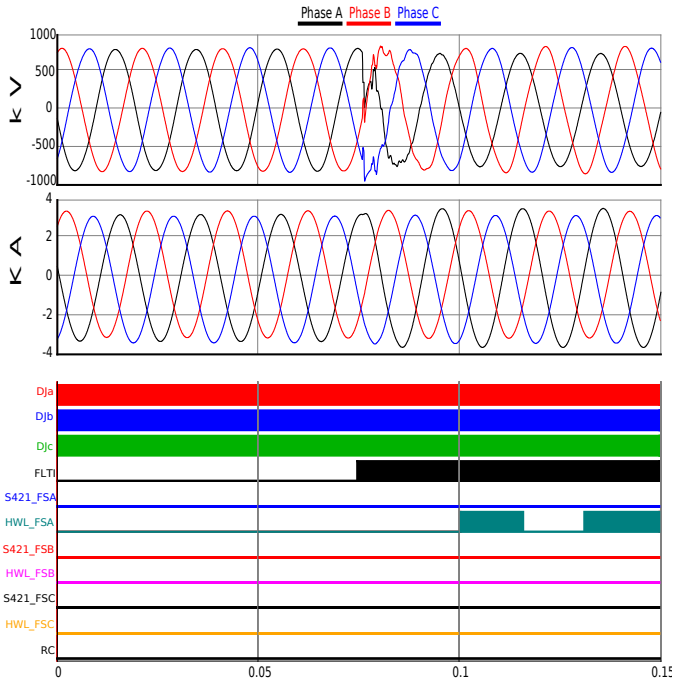

Fig. 7. Oscillography for phase A to ground fault (AG) and very week infeed condition. $Rf = 200\ \Omega$.

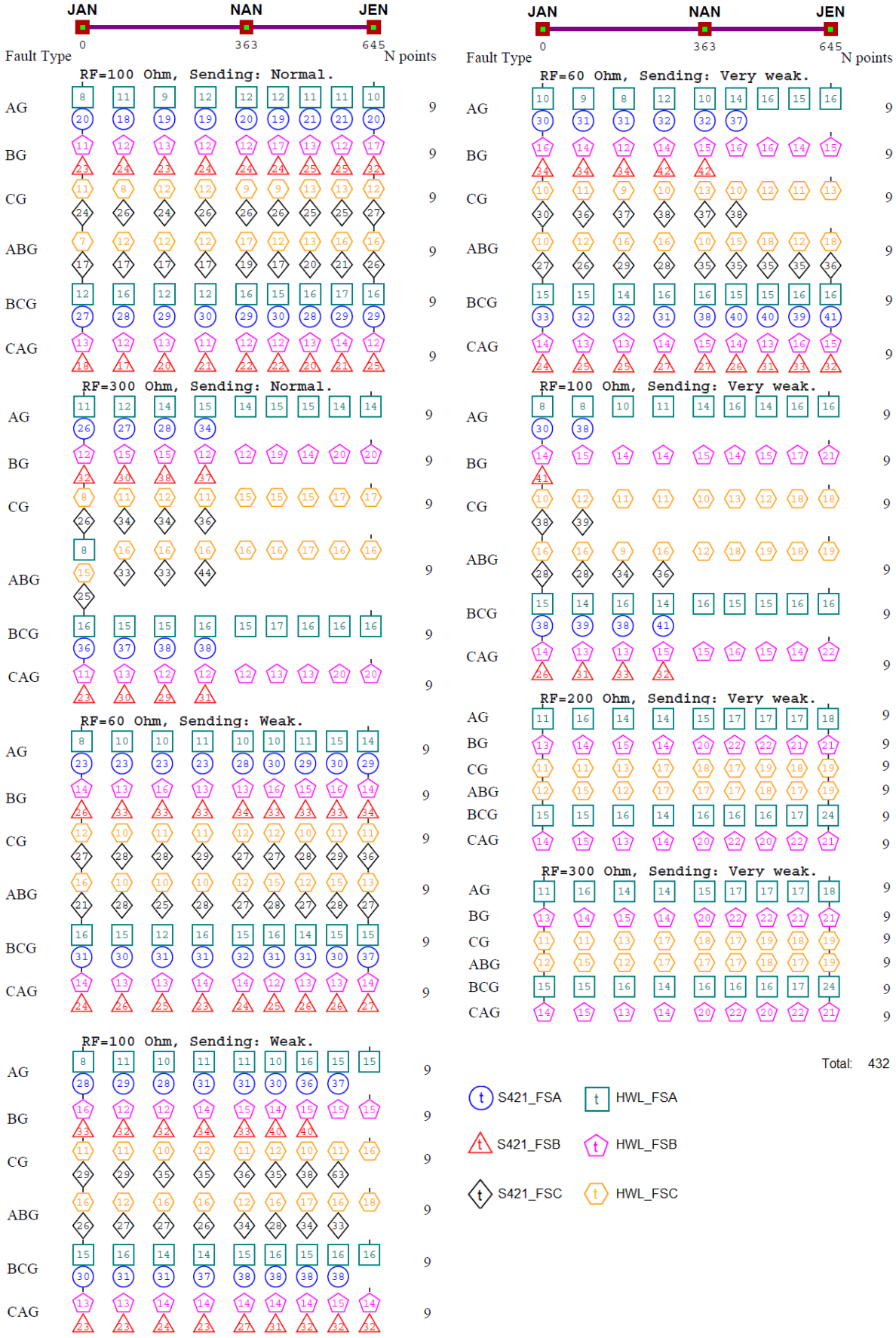

Fig. 8. Summary of bit behavior for faults along the 1000-kV UHV transmission line.

TABLE IV
SUMARY OF TIME OPERATION

Faults		HWL-FPS		SCB-FPS	
Type	N. points	N. operation	Average time [ms]	N. operation	Average time [ms]
A	72	72	12.88	38	26.05
B	72	72	15.43	35	34.11
C	72	72	12.83	38	33.12
ABG	72	72	14.89	43	28.66
BCG	72	72	15.50	43	34.66
CAG	72	72	14.85	44	26.63
Total	432	432	14.40	241	30.54

$Rf = 300\ \Omega$, it only performs well for faults in the former half on the line. Using $Zs = Zs_{min}$ (weak infeed condition) for $Rf = 100\ \Omega$, it does not perform well for faults at the end of the line. For $Zs = 2 \times Zs_{min}$ (very weak infeed condition), this algorithm only performs properly until $Rf = 60\ \Omega$. In contrast, the HWL-FPS performs correctly in all cases, including under high-resistance fault and very weak-infeed conditions. Additionally, the time responses were adequate in almost all cases.

Table IV shows an operation summary of the HWL-FPS and SCB-FPS based on Figure 8. It is possible to see that the HWL-FPS operated correctly in all cases (432), while the SCB-FPS operated correctly just for 241 cases. Additionally, the average time operation of HWL-FPS is approximately half of the SCP-FPS.

V. CONCLUSION

This study presented an application of the faulted phase selection algorithm that was originally proposed in [6] to a 1000 kV UHV 645 km long line under high-resistance and weak-infeed conditions. As it was designed using general equations for long transmission lines, without simplifications to short lines, it can be applied to lines of any length. Only a slight modification was needed in order to enhance its sensibility.

The original algorithm was developed for future very long lines (half-wavelength lines with lengths around 3200 km for a 50 Hz system), however with a minor adjustment it presents a robust response for extra long lines, as the present 630 km long one, under extreme conditions where sequence current based faulted phase selectors have poor performance. Its validity was proven through tests that were performed on a programmable relay using the RTDS real-time simulator. Many tests were performed in which faults along the line and different fault types were considered.

The proposed algorithm demonstrated satisfactory performance in almost all tests. Under extreme conditions, when conventional algorithms fail, the proposed faulted phase selector performs correctly. Thus, the robustness and the applicability of this algorithm to existent long lines that were not previously tested were proven.

REFERENCES

[1] A. Ghaderi, H. L. Ginn, and H. A. Mohammadpour, "High impedance fault detection: A review," *Electric Power Systems Research*, vol. 143, pp. 376–388, 2017. [Online]. Available: https://www.sciencedirect.com/science/article/pii/S0378779616304187

[2] Z. Y. Xu, X. Q. Yan, L. Ran, and X. Zhang, "Fault phase selection scheme of ehv/uhv transmission line protection for high-resistance faults," *IET Generation, Transmission Distribution*, vol. 6, no. 11, pp. 1180–1187, November 2012.

[3] M. R. Noori and S. M. Shahrtash, "Combined fault detector and faulted phase selector for transmission lines based on adaptive cumulative sum method," *IEEE Transactions on Power Delivery*, vol. 28, no. 3, pp. 1779–1787, July 2013.

[4] X. Wang, Z. Zhou, Y. Guo, and H. Liu, "A phase selection element for high resistance ground faults of transmission line," in *2019 IEEE Power Energy Society General Meeting (PESGM)*, 2019, pp. 1–4.

[5] S. Huang, L. Luo, and K. Cao, "A novel method of ground fault phase selection in weak-infeed side," *IEEE Transactions on Power Delivery*, vol. 29, no. 5, pp. 2215–2222, Oct 2014.

[6] R. G. Fabián and M. C. Tavares, "Faulted phase selection for half-wavelength power transmission lines," *IEEE Transactions on Power Delivery*, vol. PP, no. 99, pp. 1–1, 2017.

[7] A. A. Wolf and O. V. Scherbatchov, "Steady state operation of compensated lines with half wavelength characteristics," Tech. Rep., 1939.

[8] F. J. Hubert and M. R. Gent, "Half-wavelength power transmission lines," *IEEE Spectrum*, vol. 2, no. 1, pp. 87–92, Jan. 1965.

[9] V. Vershkov and K. T. Nakhapetyan, "Complex tests of half wavelength electrical transmission in 500 kV interconnection - USSR European CEE section," Tech. Rep., 1968.

[10] Z. Xu, S. Huang, L. Ran, J. Liu, Y. Qin, Q. Yang, and J. He, "A Distance Protection Relay for a 1000-kV UHV Transmission Line," *IEEE Transactions on Power Delivery*, vol. 23, no. 4, pp. 1795–1804, Oct. 2008.

[11] X. Lin, J. Ma, Q. Tian, and H. Weng, *Electromagnetic Transient Analysis and Novel Protective Relaying Techniques for Power Transformers*. Wiley, 2014.

[12] I. Schweitzer Engineering Laboratories, *SEL-421 Instruction manual*, 2011. [Online]. Available: http://www.selinc.com

[13] I. E. O. Schweitzar and J. Roberts, "Distance Relay Element Design," *SEL Journal of Reliable Power*, vol. 1, no. 1, 2010.